

Two-tiered Online Optimization of Region-wide Datacenter Resource Allocation via Deep Reinforcement Learning

Chang-Lin Chen, Hanhan Zhou, Jiayu Chen, Mohammad Pedramfar, Vaneet Aggarwal, Tian Lan, Zheqing Zhu, Chi Zhou, Tim Gasser, Pol Mauri Ruiz, Vijay Menon, Neeraj Kumar, and Hongbo Dong.

Abstract

This paper addresses the important need for advanced techniques in continuously allocating workloads on shared infrastructures in data centers, a problem arising due to the growing popularity and scale of cloud computing. It particularly emphasizes the scarcity of research ensuring guaranteed capacity in capacity reservations during large-scale failures. To tackle these issues, the paper presents scalable solutions for resource management. It builds on the prior establishment of capacity reservation in cluster management systems and the two-level resource allocation problem addressed by the Resource Allowance System (RAS). Recognizing the limitations of Mixed Integer Linear Programming (MILP) for server assignment in a dynamic environment, this paper proposes the use of Deep Reinforcement Learning (DRL), which has been successful in achieving long-term optimal results for time-varying systems. A novel two-level design that utilizes a DRL-based algorithm is introduced to solve optimal server-to-reservation assignment, taking into account of fault tolerance, server movement minimization, and network affinity requirements due to the impracticality of directly applying DRL algorithms to large-scale instances with millions of decision variables. This design involves a reinforcement learning agent making sequential decisions at the higher level, which are then converted into specific numbers of servers to reserve from the Main Switch Boards (MSBs). At the lower level, a heuristic approach generates the server-to-reservation mapping, considering the outcomes of the first level's reservations and environmental states. The paper explores the interconnection of these levels and the benefits of such an approach for achieving long-term optimal results in the context of large-scale cloud systems. We further show in the experiment section that our two-level DRL approach outperforms the MIP solver and heuristic approaches and exhibits significantly reduced computation time compared to the MIP solver, making it more efficient for practical implementation. Specifically, our two-level DRL approach performs 15% better than the MIP solver on minimizing the overall cost. Also, it uses only 26 seconds to execute 30 rounds of decision making, while the MIP solver needs nearly an hour.

I. INTRODUCTION

Cluster resource managers, as discussed in [1], [2], [3], play a crucial role in intelligent networks by efficiently distributing computing resources in real-time. These managers are responsible for placing and managing containers or virtual machines on servers. As cloud computing continues to gain popularity and scale, the demand for more advanced techniques to allocate workloads on shared infrastructures in data centers has grown. Specifically, the number of servers within a region can surpass millions under a hierarchical architecture, including datacenters, main switch boards, and racks [4]. Moreover, the arrival rate of workload can be up to a few thousands for a region. It is challenging to optimally place containers to servers under such large system.

Recent progress has been made in managing large-scale cluster systems. Capacity reservation aims to provide reliable capacity guarantees [5], [6]. In cloud systems, solutions have been developed to ensure capacity guarantee, considering failures at various levels such as servers, racks, and infrastructure lifecycle events like OS kernel upgrades [7]. Additionally, the cluster manager must account for workload constraints, heterogeneous hardware, and meeting service level objectives (SLOs). A resource allowance system (RAS) has been proposed in [4], which periodically solves a two-level resource allocation problem via mixed-integer programming (MIP). However, these existing work primarily focus on an offline optimization of server assignment and reservation management by considering system snapshots. They can be suboptimal for practical cluster systems that require to maximize long-term performance objectives in an online fashion, subject to various types of dynamism. While existing work have also considered the use of deep reinforcement learning (DRL) for optimizing long-term rewards through online decision-making, it often lacks scalability since training DRL algorithms for problems with a large action space (i.e., jointly over many control knobs in large-scale cluster system management) is very difficult.

To this end, this paper proposes a novel two-tiered, scalable approach for online optimization of cluster system management, which harnesses both DRL for online decision making and MIP for scalability. Specifically, we consider the problem of minimizing server movement, resource redundancy at the rack and MSB levels, and the largest failure domain, under the

Chang-Lin Chen, Jiayu Chen, Mohammad Pedramfar, and Vaneet Aggarwal are with Purdue University, West Lafayette, IN 47907 USA. E-mail: ({chen3365, chen3686, mpedramf and vaneet}@purdue.edu).

Hanhan Zhou and Tian Lan are with the George Washington University, Washington, DC 20052 USA. E-mail: ({hanhan, tlan}@gwu.edu).

Zheqing Zhu, Chi Zhou, Tim Gasser, Pol Mauri Ruiz, Vijay Menon, Neeraj Kumar, Hongbo Dong are with Meta, Menlo Park, CA 94025 USA. E-mail: ({billzhu, chizhou, timgasser, pol, vmenon, nks, hongbodong}@meta.com)

constraints of capacity guarantee and network affinity requirements. Motivated by the goal of achieving optimal results over long-run under dynamism and overcoming the limitation of RL approach for large scale system, we introduce a two-level design that utilizes a DRL-based algorithm to address the optimization problem. In the first level, a DRL agent is trained to make sequential decisions for each reservation, which are then passed to a novel action converter proposed in this paper and transformed into specific numbers of servers to reserve from the available MSBs. The DRL agent’s action affects the distribution of the servers gotten from the MSBs and the additional resource given to ensure capacity guarantee. The action converter comprising a softmax converter and an exponential converter also affects the distribution of servers from the MSBs and the capacity guarantee. In the second level, we present a low-level MILP that generates the server-to-reservation mapping, considering minimizing resource redundancy at the rack level and server movement. In this way, the DRL agent and the action converter decide the amount of additional resource supply, the distribution of servers from the MSBs and the low-level MILP gets the server-to-logical-cluster mapping considering minimizing the resource supply exceeding rack spread goal and server movement cost. The above design significantly reduces the number of variables the DRL agent has to tackle and, thus, makes training the agent more efficient.

In the experiment, several baselines include a MIP solver which RAS adopts, a complete RL which each element of its action decides whether a server is assigned to a reservation, and heuristic approaches are selected for comparison with our algorithms. The heuristic approaches adopt our two-layer design and our low-level MILP, and differ in how they determine the amount of resources to be allocated from the MSBs. We compare all the algorithms on minimizing the server movement cost, the resource spread cost, and the largest failure domain. The result shows that our algorithms achieve the lowest overall cost and subject to no constraint violations. Specifically, our proposed algorithms perform 10% and 15% better than the uniform baseline and the MIP solver on overall cost across all the percentile in 30 experiments and induce the least capacity redundancy.

II. RELATED WORKS

A. Cluster manager scheduling and solvers

Server resource allocation problems are often solved as mathematical optimization problems [8], [9], [10], [11], [12], [13], [4]. These problems involve determining the allocation of available resources, such as accelerators, servers, or network links, to clients, such as jobs, data shards, or traffic commodities, based on their specific needs. However, these mathematical optimization methods are frequently computationally expensive [14], [15]. Moreover, integer-linear programs for resource allocation problems can be even more computationally expensive [16], particularly in large-scale systems where the number of variables can reach millions (e.g., considering one variable for each client-resource pair). Consequently, the solution times for these problems can be long for solvers to generate a response (as a reference, SCS [17] requires 8 minutes to allocate a cluster with 1000 jobs [18]). Additionally, it is highly desirable for the system to make decision considering the future, it is highly desirable for the system to make decisions considering the future, while classical stochastic optimization methods developed by math programming community are usually prohibitively more expensive than deterministic problems [19]. Many existing production solutions, such as the Gavel job scheduler [20], the Accordion load balancer [21] for distributed databases, and BwE [11] for traffic engineering, can experience performance bottlenecks with an increasing number of clients and resources to allocate. Consequently, directly solving optimization problems often becomes impractical [14], leading production systems to frequently employ heuristic or meta-heuristic solutions (as in [12]) that are cheaper and faster to compute for such problems.

B. Deep Learning and Reinforcement Learning on Cluster Management

The time-varying nature and complex architecture of cloud systems make resource allocation problems challenging. Deep Reinforcement Learning (DRL) has demonstrated success in addressing dynamic and complex systems, including robotics [22], [23], [24], [25], autonomous vehicle coordination [26], [27], [28], [29], [30], communication and network packet delivery [31], [32], [33], including works through multi-agent reinforcement learning [34], [35], [36], [37]. Consequently, DRL has also been adopted to solve resource allocation problems in cloud systems. In the context of cloud systems, RL has been applied to design congestion control protocols [38] and develop simple resource management systems by treating the problem as learning packing tasks with multiple resource demands [39]. Luan et al. [40] proposed a GPU cluster scheduler that leverages DRL for intelligent locality-aware scheduling of deep learning training jobs. The authors of [41] applied RL to minimize the makespan of a job set. [42] proposed the use of actor-critic methods with input-dependent baselines for distributing computation clusters. [43] proposed a deep Q-learning approach to solve the CPU-GPU heterogeneous computing scheduling problem based on the running state and task characteristics of the cluster environment. However, it is important to note that our work significantly differs from these previous works and works in Section II-A in the aspect that we focus on optimizing server-to-logical-cluster assignment, considering failure tolerance, server movement minimization, and network affinity requirements. Then, with our solution, placing containers to servers can be more efficient since the options of each container are refined to servers more likely to satisfy the requirements.

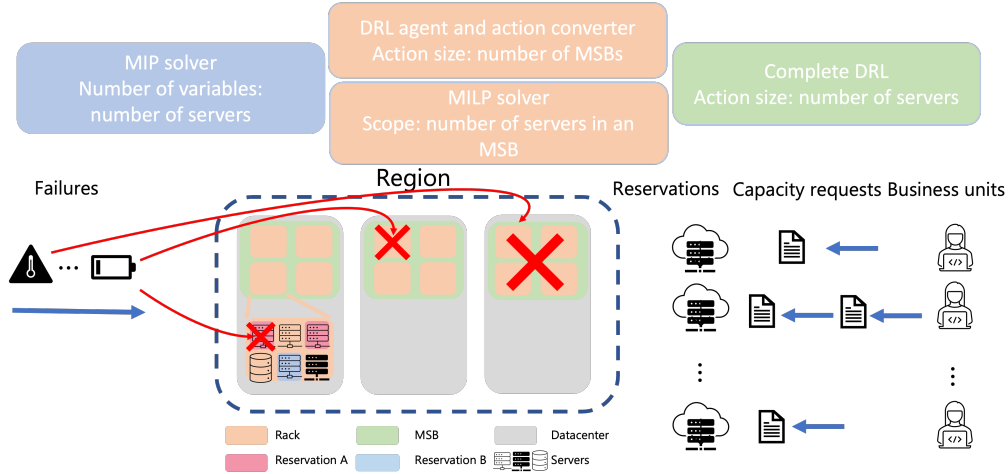


Fig. 1: Depiction of dynamic Resource Allowance System considered in this paper, as well as a brief comparison of our two-tier approach, MIP solver, and the complete RL approach. The capacity demand of a reservation is an aggregation of the capacity requests over time.

C. Capacity Reservation

A traditional approach to improving resource allocation efficiency is to group servers into physical clusters, which reduces the number of candidate servers for container placement [39], [44]. However, this method often leads to uneven utilization of clusters, suboptimal server allocation, and challenges in recovering from data center failures, causing difficulties for service owners [45]. To address these issues, the authors of [3] introduced a novel approach, Twine, by organizing servers into logistical clusters and creating a mega server pool as a backup for each logistical cluster. This design allows for flexible system management and eliminates the problem of stranded resources in small physical clusters. Building upon Twine, the Resource Allowance System (RAS) introduced in [4] further enhances resource allocation efficiency. RAS separates the server-to-logical-cluster assignment from container placement, allowing for more optimized resource allocation. It formulates the server assignment problem, considering factors such as random and correlated hardware failures, data center maintenance, and heterogeneous hardware. The problem is then periodically solved using a Mixed Integer Programming (MIP) solver.

This work focuses on achieving long-term optimum for the server-to-logical-cluster assignment, and any existing approaches can do the container placement for each logical cluster. Since system management involves a series of decision makings, optimizing the system considering only the current system status could not achieve long-term optimum. Therefore, we proposed a two-level DRL-based algorithm where a DRL agent and our proposed action converter allocate resources for each logical cluster at the MSB level, and a low-level MILP solver solves the server-to-logical-cluster mapping based on the results from the first level.

III. SYSTEM MODEL

This paper considers resource allowance system (RAS) presented in [4]. RAS abstracts the capacity of heterogeneous hardware and demand of a workload through the relative resource units (RRUs), considering a workload's relative performance on different CPUs, memory, flash, and GPUs. RAS also introduces a capacity abstraction called reservation. A reservation is a logical cluster of servers and provides capacity to the workload of a business unit. To ensure sufficient capacity for the business units, RAS optimizes the mapping between servers and reservations according to the capacity requirements, random and correlated failures, datacenter maintenance events, heterogeneous hardware resources, datacenter topology, and workload requirements. However, the complicated datacenter structures, capacity scale, and diverse workload characteristics make efficient, guaranteed capacity provision in a region challenging.

In Fig. 1, we show a region's layout overview. The datacenters in a region are connected by high-bandwidth network links. The main switch boards (MSBs) are isolated power and network domains that can fail independently. Correlated failures caused by common physical devices like power breakers and cooling fans are at the MSB level. Failures that occur at the server or rack level are considered random failures. We denote D as the set of datacenters, F as the set of MSBs, K as the set of racks, B as the set of servers, and L as a set of reservations. Considering hardware heterogeneity, the servers can be categorized into E types. In [4], users in a business unit send capacity requests to RAS, telling RAS how many additional resources they need. Then, RAS collects each reservation's capacity requests and periodically optimizes the mapping of servers and reservations.

We aim to optimize the server-to-reservation mapping in a dynamic environment. In our system, time is divided into multiple time slots with equal duration Δt . Let $\mathbb{T} = \{1, 2, \dots, t, \dots, \mathcal{T}\}$ be the set of time slots. The arrival of capacity requests for reservation l is assumed to follow the Poisson process with arrival rate λ_l . Let $\mathbf{T}_l = \{\tau_{l,1}, \tau_{l,2}, \dots\}$ be the set of capacity

requests arriving for reservation l . We denote the arrival time of the capacity request $\tau_{l,i}$ as $t_{l,i}$, its capacity demand as $\mathbf{c}_{l,i} = (c_{l,i,1}, \dots, c_{l,i,E})$ where $c_{l,i,e}$ is the demand of $\tau_{l,i}$ for server type e , and its expiration time as $t'_{l,i}$. The reservations' demand varies with time as the capacity requests come and leave. We denote $\mathbf{C}_l(t)$ as the total capacity demand of the reservation l at time t , and it is given as

$$\mathbf{C}_l(t) = \sum_{i \in \Theta_t} \mathbf{c}_{l,i} - \sum_{j \in \Theta'_t} \mathbf{c}_{l,j}, \quad (1)$$

where $\Theta_t = \{i | t_{l,i} \leq t\}$ and $\Theta'_t = \{i | t'_{l,i} \leq t\}$ are the indices of the capacity requests arriving and expiring right before time t , respectively. Note that $\mathbf{C}_l(t) = (C_{l,1}(t), \dots, C_{l,E}(t))$, where $C_{l,e}(t)$ is the capacity demand for the type e servers. According to the operation of RAS, the demand and supply of servers of one type are independent of another type.

We use an one-hot vector $\mathbf{h}_b = (h_{b,1}, \dots, h_{b,E})$ to indicate which type server b is. Let U_b be the RRU of server b and $x_{b,l}(t)$ be a binary variable equal to 1 if server b is assigned to reservation l .

a) *Server Assignment Constraint*: Assuming a server can only be assigned to one reservation at a time, servers at time slot t should satisfy the following constraint,

$$g_{1,b}(t) = 1 - \sum_{l \in L} x_{b,l}(t) \geq 0, \forall b \in B. \quad (2)$$

The objectives of RAS are to minimize server movement and optimize server spread across fault domains of various scopes.

b) *Server Movement Cost*: When RAS assigns a server to another reservation, the overhead of moving containers running on the server burdens the system. The movement cost of server b at time t is given as

$$o_{1,b}(t) = \sum_{l=1}^{|L|} M_b \times \max(0, x_{b,l}(t-1) - x_{b,l}(t)), \quad (3)$$

where M_b is the movement cost of server b .

c) *Outside Rack and MSB Goals*: For fault tolerance purposes, RAS typically assign more capacity than the reservations ask for, and aim to minimize the amount of capacity that exceeds the desired proportion of the capacity demand for each reservation and server type,

$$o_{2,k,l,e}(t) = \sum_{G \in \Psi^K} \max(0, \sum_{b \in G} (h_{b,e} \times U_b \times x_{b,l}(t)) - \alpha^K \times C_{l,e}(t)), \quad (4)$$

and

$$o_{3,f,l,e}(t) = \sum_{G \in \Psi^F} \max(0, \sum_{b \in G} (h_{b,e} \times U_b \times x_{b,l}(t)) - \alpha^F \times C_{l,e}(t)), \quad (5)$$

where Ψ^K and Ψ^F are partitions of servers based on racks and MSBs, and α^K and α^F are the spread parameters that decide the threshold for fulfilling the capacity demand within a physical scope. Making α^K and α^F small minimizes the effect of correlated and random failures on a reservation while making them large gives RAS more flexibility to optimize other objectives.

d) *Cost of Largest Failure Domain*: To minimize the impact of correlated failures, RAS also minimizes the largest amount of resources reservation l can get from the MSBs for server type e ,

$$o_{4,l,e}(t) = \max_{G \in \Psi^F} \left(\sum_{b \in G} h_{b,e} \times U_b \times x_{b,l}(t) \right), \quad (6)$$

for all l and e .

e) *Capacity Redundancy*: Moreover, to guarantee that the supply of servers of a type is enough to satisfy the capacity demand even if the MSB that provides the most capacity fails, the server-to-reservation mapping generated by RAS should satisfy the following constraint,

$$g_{2,l,e}(t) = \sum_{b \in B} (h_{b,e} \times U_b \times x_{b,l}(t)) - \max_{G \in \Psi^F} \left(\sum_{b \in G} h_{b,e} \times U_b \times x_{b,l}(t) \right) - C_{l,e}(t) \geq 0, \quad (7)$$

for all l and e .

f) *Network Affinity Requirements*: Considering that business units require different extents of network affinity, RAS uses the following constraint,

$$g_{3,d,l,e}(t) = \theta - \left| \frac{\sum_{b \in \Psi_a^D} (h_{b,e} \times U_b \times x_{b,l}(t))}{C_{l,e}(t)} - \mathbf{A}_{d,l,e} \right| \geq 0, \quad (8)$$

to enforce a reservation's preference for physical datacenters. The RAS updates the server-to-reservation assignment at the end of each time slot, considering the above objectives and constraints. We summarize the notions in Table V. The following section shows the optimization problem RAS considered and how it is optimized.

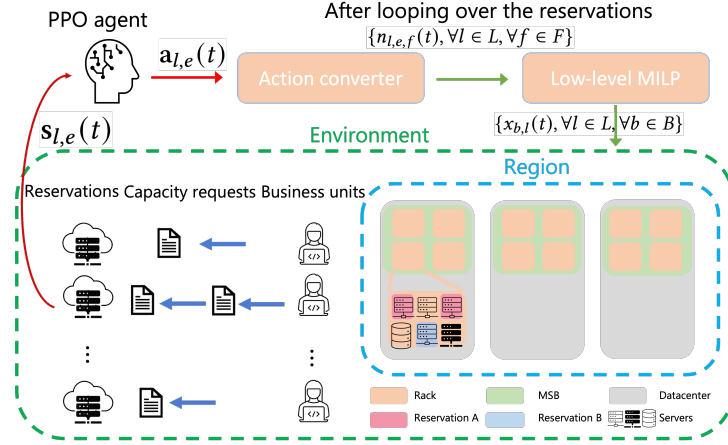


Fig. 2: A description of our proposed framework, where the PPO agent makes decisions for every reservations and then transformed into number of servers to take from the MSBs by the action converter. Finally, the numbers of servers to take from the MSBs for all reservations are converted into server-to-reservation mapping by the low-level MILP.

IV. PROBLEM FORMULATION

This section presents the problem considered in this work. RAS formulates the utility function considering the churn rate and allocation spread across MSBs and racks as,

$$\mathcal{U}(t) = \sum_{b \in B} o_{1,b}(t) + \sum_{e=1}^E \sum_{l \in L} \left(\beta \times (o_{2,l,e}(t) + o_{3,l,e}(t)) + \kappa \times o_{4,l,e}(t) \right), \quad (9)$$

where β and τ are the cost of capacity out of spread goals and the cost of correlated failure buffer capacity.

In this work, we aim to obtain long-term optimal results under dynamism considering the constraints of capacity guarantee and the network affinity requirements for each reservation. We define our Dynamic Resource Allowance System Optimization (DRASO) problem and present it as:

$$\text{DRASO : } \min_{x_{b,l}(t), \forall l \in L, b \in B, t \geq 0} \sum_{t=0}^{\infty} \gamma^t \mathcal{U}(t) \quad (10)$$

$$s.t. \quad g_{1,b,e}(t) = 1 - \sum_{l \in L} x_{b,l}(t) \geq 0, \forall b \in B, \text{ and } t \geq 0, \quad (11)$$

$$g_{2,l,e}(t) \geq 0, \forall l \in L, \text{ and } t \geq 0, \quad (12)$$

$$g_{3,d,l,e}(t) \geq 0, \forall d \in D, l \in L, \text{ and } t \geq 0, \quad (13)$$

where $\gamma \in [0, 1)$ is a discounting factor. The above problem is a mixed integer programming (MIP) problem. Note that the number of variables in DRASO can go beyond millions for a region given a time slot t . Moreover, the capacity requests which are aggregated into $C_{l,e}(t)$ and the assignment of servers can stay in the system and impact the decision-making for the next few rounds of system optimization. RAS uses a MIP solver to optimize the server-to-reservation mapping at a region level at a given t and, thus, will not give an optimal online solution. To achieve long-term optimal results, we consider adopting Reinforcement Learning (RL), widely adopted to solve sequential decision-making problems in a dynamic environment. Moreover, considering the number of variables can be very large, we combine an action converter and a low-level MILP with DRL to improve efficiency. The following section will detail each component in our proposed algorithm.

V. PROPOSED FRAMEWORK DESIGN

In this section, we present our proposed framework and hybrid DRL-based approach to solving DRASO. Our framework comprises an agent, an environment, an action converter, and a low-level MILP. In RL, an agent is trained to get long-term optimal results by sequentially evaluating its decisions sent to the environment representing our target system. The action converter and the low-level MILP are components of our approach to efficiently solving the problem. We begin with a comprehensive framework overview in Section V-A and subsequently detail each component in Sections V-B, V-C, and V-D.

Algorithm 1: Proposed algorithm

Input: $\{D, F, K, B, L, \mathcal{T}\}$
Output: $\{x_{b,l}(t), \forall b \in B, \forall l \in L\}$

```

1  $t \leftarrow 1$ 
2 repeat
3   for  $e = 1$  to  $|E|$  do
4     for  $l = 1$  to  $|L|$  do
5       Send  $s_{l,e}(t)$  to the trained PPO agent and get  $\mathbf{a}_{l,e}(t)$ 
6       Convert  $\mathbf{a}_{l,e}(t)$  to numbers of servers to take by reservation  $l$ ,  $n_{l,e,f}(t), \forall f \in F$ , by (19)
7       Get numbers of servers to take from the rack  $k$ ,  $m_{l,e,k}(t), \forall k \in K$ , by Algorithm 3
8     end
9     Get server-to-reservation mapping,  $\{x_{b,l}(t), \forall b \in B_e, \forall l \in L\}$  by Algorithm 2 and send it to the environment
10  end
11   $t \leftarrow t + 1$ 
12 until  $t == \mathcal{T}$ 

```

Algorithm 2: Description of how to get the server-to-reservation mapping for all the reservations

Input: $\{m_{l,e,k}(t), \forall l \in L, \forall k \in K\}$
Output: $\{x_{b,l}(t), \forall l \in L, \forall b \in B_e\}$

- 1 Loop through the racks to get the difference between the total requests and the capacity of the rack,
 $u_{e,k}(t) \leftarrow \sum_{r=1}^R m_{l,e,k}(t) - |\Psi_k^K|$
- 2 Loop through the racks and collect the requests to make the total requests less than the rack capacities
- 3 Loop through the collected requests to first reassign them to the racks in the same MSB they were sent to
- 4 Assign the requests that cannot be fulfilled in the previous step to any rack having vacancies
- 5 Loop through the servers to get server-to-reservation mapping

A. Framework

We start with dividing the system to decide where to apply the DRL algorithm. We find that the utility function $\mathcal{U}(t)$ in DRASO can be decoupled based on the server types and the utility function for server type e can be expressed as

$$\mathcal{U}_e(t) = \sum_{b \in B_e} o_{1,b}(t) + \sum_{l \in L} \left(\beta \times (o_{2,l,e}(t) + o_{3,l,e}(t)) + \tau \times o_{4,l,e}(t) \right), \quad (14)$$

where B_e is the set of type e servers. Moreover, as mentioned in Section III, demand of a reservation is an aggregation of multiple capacity requests which ask for multiple types of servers and can arrive and expire. As shown in Eq. (1), each tuple of the capacity demand of a reservation represents the demand for a server type, and satisfying each tuple is independent according to the RAS operation. Therefore, the utility function and the constraints can be fully decoupled according to the server types, and the optimization can be done separately for each server type.

The proposed approach for solving the optimization problem DRASO in (10) consists of two levels. In the first level, the agent is responsible for making decisions, which are then passed to the action converter to transform them into the actual number of servers to be allocated from the MSBs. In the second level, a low-level MILP is employed to determine the server-to-reservation mapping, taking into account the results obtained from the first level for all reservations and the current states of the environment.

Fig. 2 shows the basic blocks of our proposed framework and communications between them. The environment maintains the states of the servers, reservations, and capacity requests, e.g., the capacity of the reservations, previous server-to-reservation mapping, etc. These states are updated at every time slot based on the arrival and expiration of the capacity requests and the mapping decisions.

B. PPO Agent

In this section, we reframe RAS as a Markov Decision Process (MDP) that can be effectively addressed using readily available RL algorithms. For this study, we've selected PPO [46] as the algorithm because it requires less hyperparameter tuning to get satisfactory results, as well as it can generate continuous actions, and it is simple, efficient, and stable. An MDP comprises key elements such as the state space, action space, and the reward function. We present their definitions in the context of RAS as follows:

- 1) *State*: The state variables are defined to reflect the environment status and thus affect the reward feedback of different actions. We denote $s_{l,e}(t)$ as the state variable sent to the agent to decide for the reservation l and the server type e . The

state elements include the index of the reservation, the usage of the MSBs at the current time slot, the capacity demand of the reservation l , the number of servers in each MSB previously assigned to the reservation l , the amount of demand that will expire in the future h slots, and the amount of demand that will arrive in the future h time slots. In addition, the states include the mean of the other reservations' capacity demand, the number of previously assigned servers from the MSBs, to-be expired demand in the future h time slots, and demand arrivals in the future h time steps. The state elements are combined in one vector $\mathbf{s}_l(t)$.

- 2) *Action*: We denote the the agent's output for reservation l and server type e as $\mathbf{a}_{l,e}(t) = (a_{l,e,1}(t), \dots, a_{l,e,F}(t), a_{l,e,F+1}(t))$ where $\mathbf{a}_{l,e}(t) \in \mathbb{R}^{F+1}$. $\mathbf{a}_{l,e}(t)$ will be sent to the action converter. At the action converter, $a_{l,e,1}(t), \dots, a_{l,e,F}(t)$ will first be converted to the fraction of capacity demand to take from the MSBs, and $a_{l,e,F+1}(t)$ will be converted to an over-provision factor. Then, the action converter will further derive the numbers of servers of type e to take from the MSBs. $a_{l,e,1}(t), \dots, a_{l,e,F}(t)$ affect whether the servers taken are evenly from the MSBs. $a_{l,e,F+1}(t)$ determines the additional servers for the failure buffer. The conversion is detailed in Section V-C.
- 3) *Reward*: After converting a reservation's action into a server-to-reservation mapping, the reward for the reservation's action is determined by a weighted combination of the equations in the objective of the optimization problem in (10) plus penalties for violation of the constraints. The reward for reservation l at time slot t is given by

$$r_{l,e}(t) = r(\mathbf{s}_{l,e}(t), \mathbf{a}_{l,e}(t)) = w_1 \times \sum_{b \in B_e} o_{1,b}(t) + w_2 \times \sum_{k \in K} o_{2,k,l,e}(t) + w_3 \times \sum_{f \in F} o_{3,f,l,e}(t) + w_4 \times o_{4,l,e}(t) + p_{2,l,e} \times \mathbf{1}\{g_{2,l,e}(t) < 0\} + \sum_{d \in D} p_{3,d,l,e} \times \mathbf{1}\{g_{3,d,l,e}(t) < 0\} \quad (15)$$

where w_1, w_2, w_3 , and w_4 are the weights for the four equations related to reservation l in the objective, p_2 and $p_{3,d}$ are penalties for constraint violation, and $\mathbf{1}\{\cdot\}$ is an indicator function equal to 1 if the statement in the bracket holds. The penalty for violating constraints $g_{1,b}(t)$ is not included in the reward function because the proposed low-level MILP (introduced later) takes care of it. To enhance training efficiency, a progressive training approach is adopted. The agent is initially trained using only the first term of the reward function. Once the agent's performance converges, the next term is added, and the agent is retrained. This process is repeated incrementally until the agent is trained with the complete reward function. By gradually introducing the reward components, the training process becomes more efficient, allowing the agent to focus on learning each term sequentially. This approach helps in achieving convergence and improving the overall training performance.

The PPO agent takes actions sequentially for each reservation and server type according to the environment's state and learns from the records of actions, states, and rewards. The order of the decision-makings for the reservations matters in our design. The later reservations might not get enough resource to satisfy its demand. To mitigate the effect, we introduce the reservation index and the mean of the other reservations' states into the state variables, so that the agent is aware of which reservation it is making decision for and can take decisions made for other reservations into account [34]. On the contrary, the optimization of server assignment for the server types is independent of each other, so we propose the following two training methods.

- *Single agent*: We train a single agent for all the server types. To achieve this, we add the server type to the states. Following the concept of contextual MDP, we then train the agent to solve the optimization problem for a server type and move on to the next one after finishing the current training [47].
- *Parallel agents*: We train $|E|$ agents, and each is for a server type.

The Parallel agents enables faster training by parallelizing the training workload to multiple machines. We summarize the training of the PPO agent in Algorithm 5 in Appendix A.

C. Action Converter

In our system design, the PPO agent's output undergoes a sequential procedure involving our proposed action converter and low-level MILP to generate the requisite server-to-reservation mapping.

The purpose of the action converter is to determine the number of servers a reservation should get from every MSB given the actions from the PPO agent. The conversion involves converting the action to fractions of capacity to take from the MSBs and an over-provision factor and then getting the number of servers to take from the MSBs. We pass $(a_{l,e,1}(t), \dots, a_{l,e,F}(t))$, to the softmax function to get the $(a'_{l,e,1}(t), \dots, a'_{l,e,F}(t))$ as follows

$$a'_{l,e,f}(t) = \frac{e^{\zeta a_{l,e,f}(t)}}{\sum_{f \in F} e^{\zeta a_{l,e,f}(t)}}, \forall f \in F, \quad (16)$$

where ζ is the temperature parameter that affects the uniformity of $(a'_{l,e,1}(t), \dots, a'_{l,e,F}(t))$. We get the over-provision factor, $z_{l,e}(t)$, by $a_{l,e,F+1}$ and the following equation,

$$z_{l,e}(t) = \omega^{a_{l,e,F+1}(t)}, \quad (17)$$

where ω is manually set. The amount of type e resource the reservation l should get from the MSB f is given as:

$$y_{l,e,f}(t) = a'_{l,e,f}(t) \times (1 + z_{l,e}(t)) \times C_{l,e}(t). \quad (18)$$

Then, the number of type e servers that the reservation l gets from the MSB f should be:

$$n_{l,e,f}(t) = y_{l,e,f}(t) * \frac{|B_e|}{\sum_{b \in B_e} U_{b,l}}. \quad (19)$$

By (16), (17), (18) and (19), the action converter gets the number of servers a reservation should get from the MSBs.

D. Integration with the Low-level MILP

With the results from the action converter, our low-level MILP derives the server-to-reservation mapping. Since the resource spread across the MSBs and the maximum correlated failure are handled by the PPO agent, our low-level MILP is designed to minimize the movement cost of servers in (11) and the resource spread across the racks in (4). The two essential steps in our low-level MILP to get the server-to-reservation mapping are as follows:

- 1) Given the number of servers the reservation l should get from the MSB f , $n_{l,e,f}(t)$, the reservation l gets an even number of servers from the racks in the MSB f . We use Algorithm 3 to decide how many servers the reservation l should get from all the racks.
- 2) Based on the number of servers every reservation should take from the MSBs, we can get the server-to-reservation mapping. The detailed steps are shown in Algorithm 2, and the corresponding pseudocode can be found in Algorithm 4 in A.

VI. SIMULATION

We evaluate the performance of our proposed algorithm in this section. We begin with the system setup in Section VI-A, clarify the baselines in Section VI-B, and show the performance comparison in Section VI-C.

A. System Setup

Table I delineates the key parameters of our Resource Allowance System (RAS). The counts of datacenters, MSBs, racks, reservations, servers, and server types are symbolized as $|D|$, $|F|$, $|K|$, $|L|$, $|B|$, and $|E|$, respectively. These symbols illustrate the regional datacenter topology depicted in Fig. 1. U_b , representing the RRU of server b , is unified since most of the servers of the same server type are homogeneous. This datacenter setup is designed by domain experts among the authors, approximating a real-life scenario. For one experiment/episode, we run the system for 30 steps. The other parameters in Table I are related to the optimization problem, of which the definitions are provided in Table V.

TABLE I: Parameter Setup

Parameter	$ D $	$ F $	$ K $	$ L $	$ B $	$ E $	U_b	T	α^F	α^K	κ	β	M_b	$A_{l,d}$	θ
Value	3	15	75	20	1000	10	150	30	1/15	1/75	1	1	5	1	2

The regional datacenter comprises 1000 servers, differentiated into 10 types based on count, mean request arrival rate, and capacity combination type. A comprehensive summary of this heterogeneous simulation setting, designed by domain experts, is provided in Table II.

TABLE II: Summary of the Heterogeneous Hardware

Server Type	0	1	2	3	4	5	6	7	8	9
Count	405	45	30	15	300	15	30	15	45	100
Mean Request Arrival Rate	2	0.6	0.6	0.2	1.8	0.2	0.6	0.2	0.6	1.2
Capacity Combination Type	5	2	1	0	4	1	2	1	2	3

There are in total 6 types of capacity combinations. Each type corresponds to a unique amalgamation of demands varying in size or duration, which is summarized in Table III. The hardwares are evenly distributed in their higher scopes *e.g.*, the racks have the same number of servers, and the MSBs have the same number of racks. We build a simulator in Python based on the described settings.

TABLE III: Summary of Different Capacity Requests

Capacity Combination Type	0	1	2	3	4	5
Demands	(150)	(300, 150)	(300, 150)	(300, 150)	(450, 300)	(900, 450, 150)
Percentage	(1.00)	(0.16, 0.84)	(0.25, 0.75)	(0.33, 0.67)	(0.33, 0.67)	(0.16, 0.33, 0.51)
Duration	(15)	(10, 15)	(10, 15)	(10, 15)	(10, 15)	(10, 15, 20)

B. Baseline Algorithms

This section describes the baseline algorithms. We include the MIP solver, which RAS currently adopts, a complete RL agent, and some two-layer heuristic methods. The descriptions of the baseline algorithms are given as follows.

- MIP solver: It is implemented by the Python-MIP package [48]. The MIP solver is configured to spend at most 10 seconds to solve a problem.
- Complete RL/vanilla: The action space of the agent is equal to the set of variables in (10), where each output of the agent is then converted to 0 or 1 to represent $x_{b,i}(t)$. We use the PPO algorithm to train the agent.
- Random: It uniformly samples $|F|$ weights and an over-provision factor from the range $[-1, 1]$. Then, the $|F| + 1$ values are sent to the action converter and our low-level MILP to get the server-to-reservation mapping.
- Uniform: Let the fractions of capacity demand to take from the MSBs be $\frac{1}{|F|-1}$. The choice of the fraction will make (7) satisfied. The fractions are sent to the action converter and our low-level MILP to obtain the server-to-reservation mapping.
- Proportional: It first generates F scalars, $\delta_1, \dots, \delta_F$, proportional to the available resource of the MSBs. Assume that $(\delta_1, \dots, \delta_F)$ are in the descending order and they sum to one. Then, multiply all the scalars by $\frac{1}{1-\delta_1}$ to satisfy (7). Finally, the scalars are sent to the action converter and our low-level MILP to get the server-to-reservation mapping.

C. Main Results

We compare the performance of our proposed algorithms with the baseline algorithms in this section. The convergence rate of our proposed algorithm is presented in Figure 3. In Figures 4, 5, and 6, we compare the baselines and our algorithm on the overall performance, resulting in server movement cost, spread, size of the largest fault domain, and induced capacity redundancy. We tested the performance as the system scale increases in Table IV. Finally, we discuss the relationship between the terms in the objective function in Figure 7.

We first show the convergence rate in terms of the number of episodes required to reach convergence. In Figures 3a and 3b, we train the agent for server type 1 for 400 episodes. Figure 3a shows the variation of the reward and its moving average. We observe that the moving average converges after 100 episodes. Similarly, in Figure 3b, we observe that there is little variation of the moving average of the objective value and constraint 6 after 100 episodes. Training plots for the rest server types are omitted for the sake of repetition.

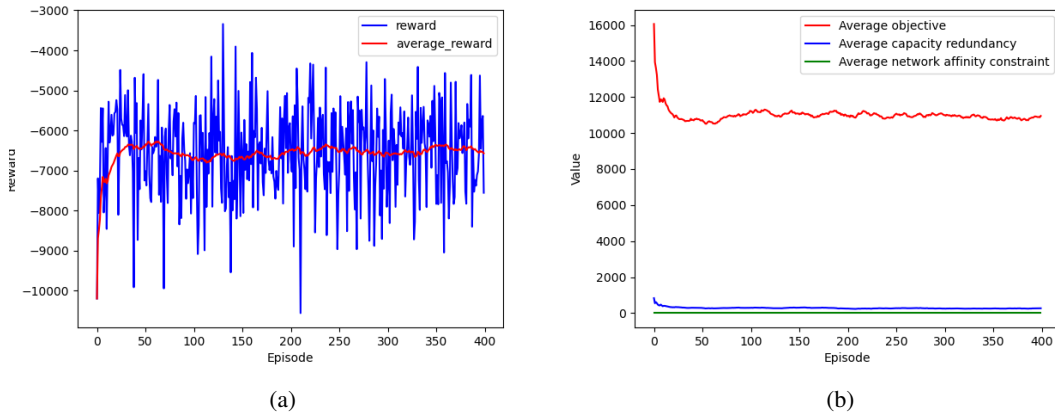


Fig. 3: Algorithm convergence simulations for the server type 1. Both our proposed parallel agents and our proposed single agent algorithms show similar convergence pattern. The result shows that the moving average of the reward, the objective value, the capacity redundancy constraint, and the network affinity constraint of our proposed algorithms converge after 100 episodes.

In Figures 4, 5, 6, we compare the overall performance, key metrics, and the resource utilization of the algorithms based on 30 episodes of the performance data. Two kinds of plots are used to show the performance difference. The first kind compares the empirical cumulative distribution function (CDF) of a metric, where the horizontal axis represents the metric value and the

vertical axis represents the percentile. The second kind compares the performance induced at each time step within an episode, where the horizontal axis represents the time steps and the vertical axis represents the metric values.

In Figure 4a and 4b, we compare the empirical CDF of the resulting objective value. Because the complete RL and the random baseline performs much worse than the other algorithms, we divide the comparison into two figures for better comparison. A lower objective value is desired as it indicates better performance. The horizontal axis represents the objective value accumulated in an episode, while the vertical axis represents the percentile of an episode’s accumulated objective value among all the episodes’ objective values generated by a specific algorithm. The overall performance of the two proposed algorithms is very close, indicating that using a single agent can achieve similar performance to using parallel agents. The uniform and proportional baselines show similar performance. This can be attributed to the fact that the initial outputs of the proportional baseline are always uniform. The slight differences in their outputs may not significantly affect the generated server-to-reservation mappings by the action converter. The proposed algorithms consistently achieve the lowest objective values across all percentiles, outperforming the baselines. This demonstrates the effectiveness of the proposed algorithms in optimizing the objective function. The medians of our proposed algorithms, the uniform and proportional baselines, and the MIP solver are 38000, 42000, and 44000, respectively, to name a few. The objective value obtained by complete RL ranges from 90000 to 130000, which indicates that the training of the complete RL converges at a suboptimal point and verifies that training an RL agent directly for a large-scale system is impractical. Since the complete RL and the random baseline performs much worse than the others, we omit their performance comparison with the proposed algorithms for the following content.

In Figure 4c, the variation of the objective value within an episode is depicted, providing a different perspective for comparing performance. The horizontal axis represents the time steps within an episode, while the vertical axis displays the corresponding objective value. As the time steps within an episode increase, the performance difference between the proposed algorithms and the baseline algorithms becomes more pronounced. This suggests that the proposed algorithms exhibit better optimization capabilities and consistently improve the objective value over time compared to the baseline algorithms. Figure 4c supports the conclusion made in Figure 4a, reinforcing the finding that the proposed algorithms outperform the baselines in terms of objective value optimization. We can conclude that our proposed algorithm performs better than the proportional baseline and the MIP by 10% and 15%, respectively, at the median of the experiments.

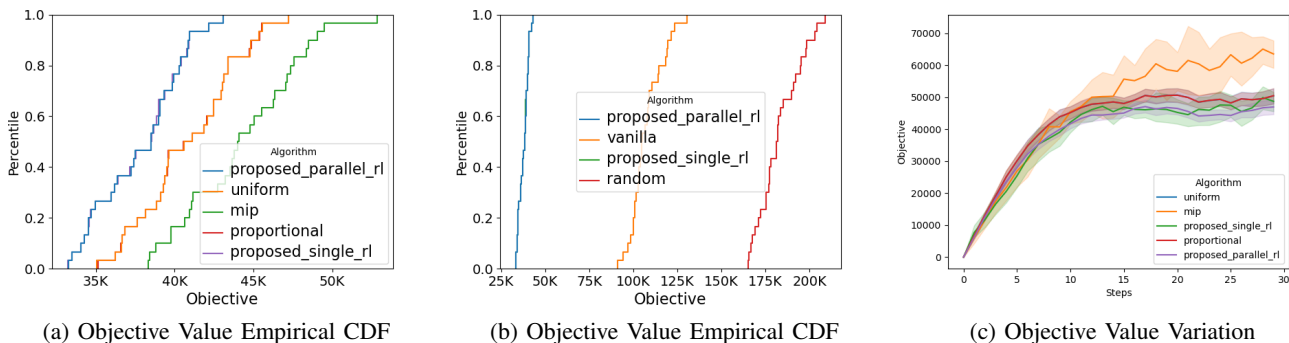


Fig. 4: Performance comparison with regards to the objective value ($\mathcal{U}(t)$). Lower objective value and outside MSB goal are desired. The results shows that our proposed algorithms outperform the other algorithms in the sense that (a) (b) they result in the lowest objective value across all the percentile, and (c) their average remain the lowest within an episode.

Figure 5a illustrates that both the uniform and proportional baselines result in the lowest server movement cost. Additionally, the two proposed algorithms outperform the MIP solver significantly in terms of server movement cost. The results of the uniform and proportional baselines imply that uniformly getting resources for all the scopes renders the least server movement cost. However, the objective function of the problem is primarily influenced by the resource spread components as demonstrated in Figures 5b and 4. Figure 5c shows that all the algorithms maintain the largest failure domain equally well. It implies that these algorithms are comparable in terms of their ability to handle failures effectively.

We can also observe that our proposed algorithms use the least extra resource to satisfy the demand from Figures 6a and 6b. The results in Figures 6a and 6b accord with what we deduce from Figure 5b. Besides the overall induced capacity redundancy, we also show the capacity redundancy violation in Figure 6c which cannot be observed from Figures 6a and 6b. Figure 6c shows that the proportional and uniform baselines violates the capacity redundancy constraint starting at step 5 till the end. Note that we design the outputs of the uniform and proportional to satisfy the capacity redundancy constraint. We deduce that the violation might be due to competition of the servers when the demand increases. In our low-level MILP, server requests which cannot be fulfilled because of rack capacity limit will be redistribute to other racks, and our low-level MILP does not guarantee constraint satisfaction when redistribution has to be made. We can also conclude that our proposed agent can learn to avoid constraint violation.

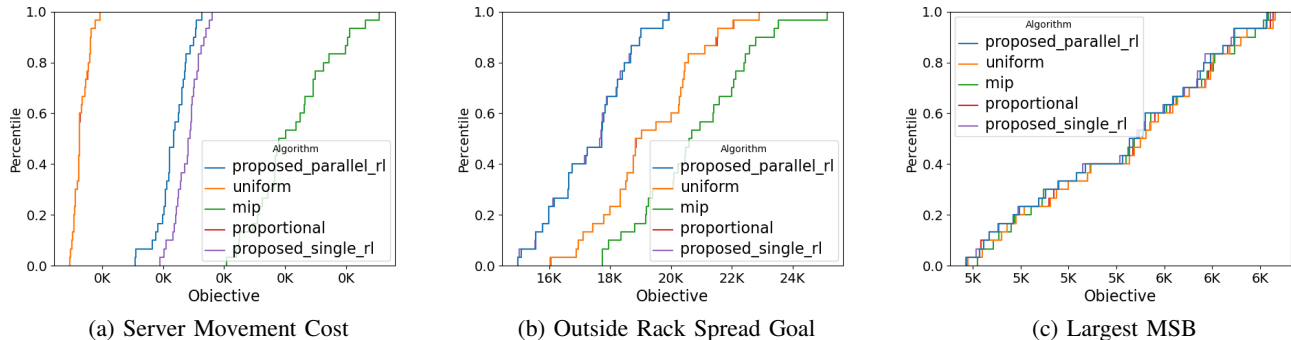


Fig. 5: The empirical CDF comparison concludes that (a) the proportional and uniform baselines induce the least server movement cost, (b) our proposed algorithms use the least resource outside rack spread goal, and (c) all the algorithms perform equally well in maintaining the size of the largest MSB.

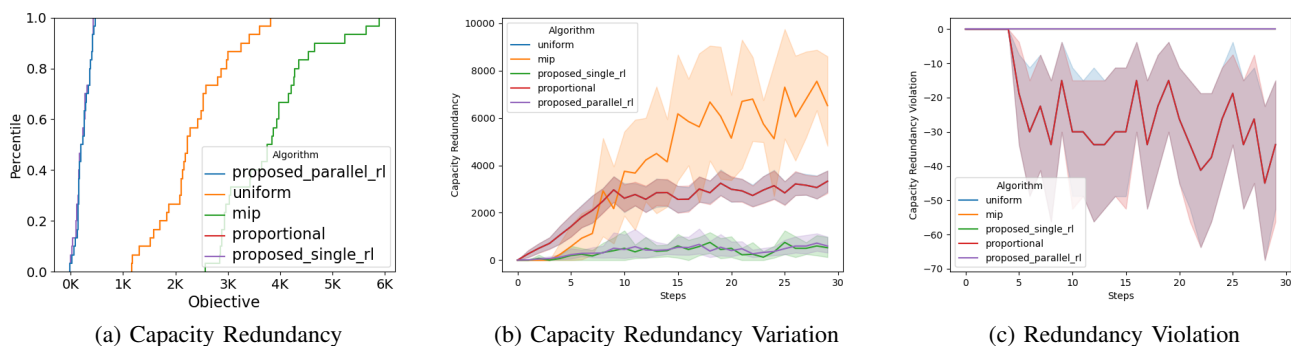


Fig. 6: We conclude that the resource utilization of our proposed algorithms is the most efficient and reliable by (a) their capacity redundancy is the lowest across the percentile, (b) their average capacity redundancy is the lowest for all time steps in an episode, and (c) they do not violate the redundancy constraint.

Table IV compares the scalability of the proposed single agent algorithm with the MIP solver based on testing time and training time, measured on the same machine with 32 CPU cores and 64 GB RAM. The table includes results for varying numbers of servers, ranging from 500 to 10,000. Testing time represents the time required to finish one episode, *i.e.*, 30 consecutive decision-makings. On the other hand, the training time is the expected time for training our RL agent for 1000 episodes. The testing time in Table IV are averaged over 30 episodes, while the training time represents the time required to train the agent for 1000 episodes. Our proposed algorithm shows manageable training times even with a system containing 10000 servers. Moreover, the proposed algorithm exhibits significantly lower testing times compared to the MIP solver, highlighting greater flexibility in system management. Though the training time may take hours or even days for very large system, most of the training needs can be anticipated and planned in advance. Moreover, updating the RL model is simple and convenient. Besides the training and testing time, our proposed algorithm also outperforms the MIP as indicated by both the table and the previous figures. Note that the training time for our proposed parallel agents algorithm can be further reduced by training each model on different devices simultaneously. The training time of the proposed parallel agents can be 14, 36, 56 minutes for systems with 500, 1000, and 10000 servers, respectively.

TABLE IV: Summary of the algorithm scalability

(Algorithm, $ B $)	(MIP, 500)	(MIP, 1000)	(Proposed, 500)	(Proposed, 1000)	(Proposed, 10000)
Testing time (sec)	2329	3510	10	26	39
Training time (min)	N/A	N/A	53	142	224
Performance $\mathcal{U}(t)$	25746	44213	21128	37795	1221747

In Figures 7, we examine the trade-off between metrics in the optimization problem as the server movement cost (M_b) increases. Since the single agent algorithm and parallel agents algorithm have close performance, we test only the performance of the single agent. We plot Figure 7 based on 5 episodes of performance data obtained at different server movement costs: 5, 10, 25, and 50. Figure 7a indicates that the total number of server movement decreases as the server movement cost increases.

We also observe slight rise on the resource spread and capacity redundancy as shown in Figures 7a and 7b. This increase might be due to the utilization of additional servers to satisfy incoming demands and avoid the high server movement cost.

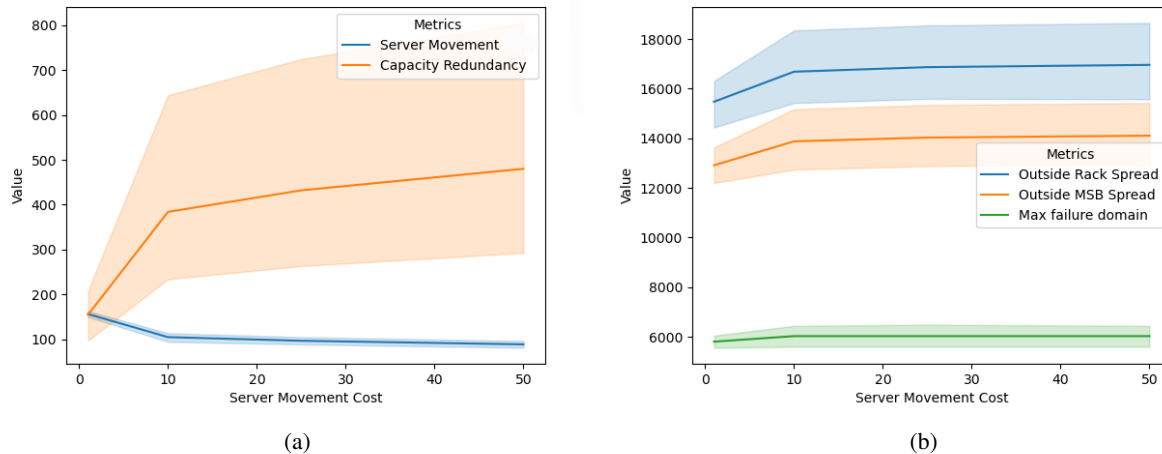


Fig. 7: The increase of the server movement cost helps further minimize the server movements, but induces higher capacity redundancy and worse resource spread.

VII. CONCLUSION

This work considers optimizing server-to-reservation mapping for a dynamic reservation allowance system (RAS) constituting datacenters, MSBs, racks, and heterogeneous servers. At the first level, a DRL agent and an action converter collaboratively determine the resource supply for each reservation sequentially at the MSB level. The outputs from this level are then passed to the second level, where a low-level MILP is employed to solve the server-to-reservation mapping problem based on the results obtained from the first level. To handle the heterogeneity of the servers, the optimization problem is initially decoupled according to the different server types. This allows for independent optimization for each server type, simplifying the overall problem. Two variants of the proposed algorithm are presented: one utilizing a single DRL agent and the other employing parallel agents for the DRL part. Both variants are evaluated and compared with other algorithms, including heuristic approaches and the Mixed Integer Programming (MIP) solver utilized in the RAS. Simulation results demonstrate that the proposed algorithms outperform the other methods in terms of performance. Additionally, the proposed algorithms exhibit significantly reduced computation time compared to the MIP solver, making them more efficient for practical implementation. Future steps for this work include extending the optimization problem to incorporate practical failure arrivals and addressing containers' placement on servers to satisfy specific service requirements. These extensions would further enhance the practical applicability and effectiveness of the proposed algorithms in real-world scenarios.

REFERENCES

- [1] A. Verma, L. Pedrosa, M. R. Korupolu, D. Oppenheimer, E. Tune, and J. Wilkes, "Large-scale cluster management at Google with Borg," in *Proceedings of the European Conference on Computer Systems (EuroSys)*, Bordeaux, France, 2015.
- [2] B. Hindman, A. Konwinski, M. Zaharia, A. Ghodsi, A. D. Joseph, R. Katz, S. Shenker, and I. Stoica, "Mesos: A platform for Fine-Grained resource sharing in the data center," in *8th USENIX Symposium on Networked Systems Design and Implementation (NSDI 11)*. Boston, MA: USENIX Association, Mar. 2011.
- [3] C. Tang, K. Yu, K. Veeraraghavan, J. Kaldor, S. Michelson, T. Kooburat, A. Anbudurai, M. Clark, K. Gogia, L. Cheng *et al.*, "Twine: A unified cluster management system for shared infrastructure," in *Proceedings of the 14th USENIX Conference on Operating Systems Design and Implementation, 2020*, pp. 787–803.
- [4] A. Newell, D. Skarlatos, J. Fan, P. Kumar, M. Khutornenko, M. Pundir, Y. Zhang, M. Zhang, Y. Liu, L. Le *et al.*, "Ras: continuously optimized region-wide datacenter resource allocation," in *Proceedings of the ACM SIGOPS 28th Symposium on Operating Systems Principles*, 2021, pp. 505–520.
- [5] AWS. (2023) On-demand capacity reservations. [Online]. Available: <https://docs.aws.amazon.com/AWSEC2/latest/UserGuide/ec2-capacity-reservations.html>
- [6] Google. (2023) Reservations of compute engine zonal resources. [Online]. Available: <https://cloud.google.com/compute/docs/instances/reservations-overview>
- [7] A. Verbitski, A. Gupta, D. Saha, M. Brahmadesam, K. Gupta, R. Mittal, S. Krishnamurthy, S. Maurice, T. Kharatishvili, and X. Bao, "Amazon aurora: Design considerations for high throughput cloud-native relational databases," in *SIGMOD 2017*, 2017.
- [8] F. Abuzaid, S. Kandula, B. Arzani, I. Menache, M. Zaharia, and P. Bailis, "Contracting wide-area network topologies to solve flow problems quickly," in *NSDI*, 2021, pp. 175–200.
- [9] Y. Xiang, T. Lan, V. Aggarwal, and Y.-F. R. Chen, "Joint latency and cost optimization for erasure-coded data center storage," *IEEE/ACM Transactions on Networking*, vol. 24, no. 4, pp. 2443–2457, 2015.
- [10] I. Gog, M. Schwarzkopf, A. Gleave, R. N. Watson, and S. Hand, "Firmament: Fast, centralized cluster scheduling at scale," in *12th USENIX Symposium on Operating Systems Design and Implementation (OSDI 16)*, 2016, pp. 99–115.
- [11] A. Kumar, S. Jain, U. Naik, A. Raghuraman, N. Kasinadhuni, E. C. Zermeno, C. S. Gunn, J. Ai, B. Carlin, M. Amarandei-Stavila *et al.*, "Bwe: Flexible, hierarchical bandwidth allocation for wan distributed computing," in *Proceedings of the 2015 ACM Conference on Special Interest Group on Data Communication*, 2015, pp. 1–14.

- [12] F. Stefanello, V. Aggarwal, L. S. Buriol, and M. G. Resende, "Hybrid algorithms for placement of virtual machines across geo-separated data centers," *Journal of Combinatorial Optimization*, vol. 38, pp. 748–793, 2019.
- [13] X. Li and K. L. Yeung, "Traffic engineering in segment routing networks using milp," *IEEE Transactions on Network and Service Management*, vol. 17, no. 3, pp. 1941–1953, 2020.
- [14] D. Narayanan, F. Kazhmiaka, F. Abuzaid, P. Kraft, A. Agrawal, S. Kandula, S. Boyd, and M. Zaharia, "Solving large-scale granular resource allocation problems efficiently with pop," in *Proceedings of the ACM SIGOPS 28th Symposium on Operating Systems Principles*, 2021, pp. 521–537.
- [15] Y. Mei, H. Zhou, and T. Lan, "Remix: Regret minimization for monotonic value function factorization in multiagent reinforcement learning," *arXiv preprint arXiv:2302.05593*, 2023.
- [16] Y. T. Lee and A. Sidford, "Efficient inverse maintenance and faster algorithms for linear programming," in *2015 IEEE 56th Annual Symposium on Foundations of Computer Science*. IEEE, 2015, pp. 230–249.
- [17] B. O'Donoghue, E. Chu, N. Parikh, and S. Boyd, "SCS: Splitting conic solver, version 3.2.3," <https://github.com/cvxgrp/scs>, Nov. 2022.
- [18] B. O'donoghue, E. Chu, N. Parikh, and S. Boyd, "Conic optimization via operator splitting and homogeneous self-dual embedding," *Journal of Optimization Theory and Applications*, vol. 169, pp. 1042–1068, 2016.
- [19] A. Shapiro and A. Philpott, "A tutorial on stochastic programming," *Manuscript. Available at www2.isye.gatech.edu/ashapiro/publications.html*, vol. 17, 2007.
- [20] D. Narayanan, K. Santhanam, F. Kazhmiaka, A. Phanishayee, and M. Zaharia, "Heterogeneity-aware cluster scheduling policies for deep learning workloads," in *Proceedings of the 14th USENIX Conference on Operating Systems Design and Implementation*, 2020, pp. 481–498.
- [21] M. Serafini, E. Mansour, A. Aboulnaga, K. Salem, T. Rafiq, and U. F. Minhas, "Accordion: Elastic scalability for database systems supporting distributed transactions," *Proceedings of the VLDB Endowment*, vol. 7, no. 12, pp. 1035–1046, 2014.
- [22] H. Nguyen and H. La, "Review of deep reinforcement learning for robot manipulation," in *IEEE International Conference on Robotic Computing (IRC)*, 2019, pp. 590–595.
- [23] J. Chen, T. Lan, and V. Aggarwal, "Option-aware adversarial inverse reinforcement learning for robotic control." IEEE, 2023.
- [24] J. Chen, D. Tamboli, T. Lan, and V. Aggarwal, "Multi-task hierarchical adversarial inverse reinforcement learning," 2023.
- [25] H. Zhou, T. Lan, and V. Aggarwal, "Value functions factorization with latent state information sharing in decentralized multi-agent policy gradients," *arXiv preprint arXiv:2201.01247*, 2022.
- [26] Y. Hu, A. Nakhai, M. Tomizuka, and K. Fujimura, "Interaction-aware decision making with adaptive strategies under merging scenarios," in *2019 IEEE/RSJ International Conference on Intelligent Robots and Systems (IROS)*. IEEE, 2019, pp. 151–158.
- [27] A. O. Al-Abbasi, A. Ghosh, and V. Aggarwal, "Deepool: Distributed model-free algorithm for ride-sharing using deep reinforcement learning," *IEEE Transactions on Intelligent Transportation Systems*, vol. 20, no. 12, pp. 4714–4727, 2019.
- [28] X. Luo, X. Ma, M. Munden, Y.-J. Wu, and Y. Jiang, "A multisource data approach for estimating vehicle queue length at metered on-ramps," *Journal of Transportation Engineering, Part A: Systems*, vol. 148, no. 2, p. 04021117, 2022.
- [29] X. Ma, "Traffic performance evaluation using statistical and machine learning methods," Ph.D. dissertation, The University of Arizona, 2022.
- [30] J. Chen, A. K. Umrawal, T. Lan, and V. Aggarwal, "Deepfreight: A model-free deep-reinforcement-learning-based algorithm for multi-transfer freight delivery," in *Proceedings of the International Conference on Automated Planning and Scheduling*, vol. 31, 2021, pp. 510–518.
- [31] D. Ye, M. Zhang, and Y. Yang, "A multi-agent framework for packet routing in wireless sensor networks," *sensors*, vol. 15, no. 5, pp. 10026–10047, 2015.
- [32] N. Geng, Q. Bai, C. Liu, T. Lan, V. Aggarwal, Y. Yang, and M. Xu, "A reinforcement learning framework for vehicular network routing under peak and average constraints," *IEEE Transactions on Vehicular Technology*, 2023.
- [33] G. Gonzalez, M. Balakuntala, M. Agarwal, T. Low, B. Knoth, A. W. Kirkpatrick, J. McKee, G. Hager, V. Aggarwal, Y. Xue *et al.*, "Asap: A semi-autonomous precise system for telesurgery during communication delays," *IEEE Transactions on Medical Robotics and Bionics*, vol. 5, no. 1, pp. 66–78, 2023.
- [34] W. U. Mondal, V. Aggarwal, and S. V. Ukkusuri, "Can mean field control (mfc) approximate cooperative multi agent reinforcement learning (marl) with non-uniform interaction?" in *Uncertainty in Artificial Intelligence*. PMLR, 2022, pp. 1371–1380.
- [35] H. Zhou, T. Lan, and V. Aggarwal, "Pac: Assisted value factorization with counterfactual predictions in multi-agent reinforcement learning," in *Advances in Neural Information Processing Systems*, vol. 35. Curran Associates, Inc., 2022, pp. 15757–15769.
- [36] D. S. Gadiraju, V. Lalitha, and V. Aggarwal, "An optimization framework based on deep reinforcement learning approaches for prism blockchain," *IEEE Transactions on Services Computing*, 2023.
- [37] Y. Mei, H. Zhou, T. Lan, G. Venkataramani, and P. Wei, "Mac-po: Multi-agent experience replay via collective priority optimization," in *Proceedings of the 2023 International Conference on Autonomous Agents and Multiagent Systems*, ser. AAMAS '23. International Foundation for Autonomous Agents and Multiagent Systems, 2023, p. 466–475.
- [38] K. Winstein and H. Balakrishnan, "Tcp ex machina: Computer-generated congestion control," *ACM SIGCOMM Computer Communication Review*, vol. 43, no. 4, pp. 123–134, 2013.
- [39] H. Mao, M. Alizadeh, I. Menache, and S. Kandula, "Resource management with deep reinforcement learning," in *Proceedings of the 15th ACM workshop on hot topics in networks*, 2016, pp. 50–56.
- [40] Y. Luan, X. Chen, H. Zhao, Z. Yang, and Y. Dai, "Sched²: Scheduling deep learning training via deep reinforcement learning," in *2019 IEEE Global Communications Conference (GLOBECOM)*. IEEE, 2019, pp. 1–7.
- [41] F. Li and B. Hu, "Deepjs: Job scheduling based on deep reinforcement learning in cloud data center," in *Proceedings of the 4th International Conference on Big Data and Computing*, 2019, pp. 48–53.
- [42] H. Mao, M. Schwarzkopf, S. B. Venkatakrishnan, Z. Meng, and M. Alizadeh, "Learning scheduling algorithms for data processing clusters," in *Proceedings of the ACM special interest group on data communication*, 2019, pp. 270–288.
- [43] H. Zhang, X. Geng, and H. Ma, "Learning-driven interference-aware workload parallelization for streaming applications in heterogeneous cluster," *IEEE Transactions on Parallel and Distributed Systems*, vol. 32, no. 1, pp. 1–15, 2020.
- [44] C.-L. Chen, C. G. Brinton, and V. Aggarwal, "Latency minimization for mobile edge computing networks," *IEEE Transactions on Mobile Computing*, vol. 22, no. 4, pp. 2233–2247, 2023.
- [45] S. Swarup, E. M. Shakshuki, and A. Yasar, "Task scheduling in cloud using deep reinforcement learning," *Procedia Computer Science*, vol. 184, pp. 42–51, 2021.
- [46] J. Schulman, F. Wolski, P. Dhariwal, A. Radford, and O. Klimov, "Proximal policy optimization algorithms," *CoRR*, vol. abs/1707.06347, 2017.
- [47] A. Hallak, D. Di Castro, and S. Mannor, "Contextual markov decision processes," *arXiv preprint arXiv:1502.02259*, 2015.
- [48] H. G. S. Túlio A. M. Toffolo. (2019) Python-mip. [Online]. Available: <https://www.python-mip.com>

APPENDIX

A. NOMENCLATURE

Table V. below summarizes the common notations used in this paper.

TABLE V: Summary of Optimization Problem Parameters

Notation	Description
D	Set of datacenters
F	Set of MSBs
K	Set of racks
B	Set of servers
L	Set of all reservations
E	Set of server types
$x_{b,l}(t)$	Assignment variable which is 1 if server b is assigned to reservation l and 0 otherwise
$\alpha_b(t)$	The reservation that server b is assigned to at time slot t
M_b	Movement cost of server b
κ	Cost of each correlated-failure-buffer server
β	Cost of each server outside of spread goals
$\alpha^{K,F}$	Proportional limit of reservation of spread in K (rack) or F (MSB fault domain)
U_b	RRU of server b
$C_l(t)$	Capacity desired for reservation l
$\Psi^{K,F,D}$	Partition of servers based on K (rack), D (datacenter), or F (MSB fault domain)
$\Psi_k^K, \Psi_f^F, \Psi_d^D$	Servers in rack k , in MSB f , or in datacenter d
Φ_f^F	Racks in MSB F (MSB fault domain)
$A_{d,l,e}$	Affinity of reservation l to a datacenter regarding server type e

Algorithm 3: Get the number of servers to take from the racks in MSBs for reservations

Input: $r, \{n_{l,e,f}(t), \forall l \in L, \forall f \in F\}$

Output: $\{m_{l,e,k}(t), \forall l \in L, \forall k \in K\}$ — the number of servers reservation l should take from the racks.

```

1 for  $f = 1$  to  $|F|$  do
2   Sort the racks in the MSB  $f$  according to the number of servers previously assigned to reservation  $l$  in the
   descending order
3    $p \leftarrow$  quotient of  $n_{l,e,f}(t)$  by the number of racks in MSB  $f$ 
4    $q \leftarrow$  modulus of  $n_{l,e,f}(t)$  by the number of racks in MSB  $f$ 
5    $counter \leftarrow 0$ 
6   for  $k$  in  $\Phi_f^F$  do
7     if  $counter < q$  then
8        $m_{l,e,k}(t) \leftarrow p + 1$ 
9     else
10       $m_{l,e,k}(t) \leftarrow p$ 
11    end
12     $counter \leftarrow counter + 1$ 
13  end
14 end

```

Algorithm 4: Pseudocode of Algorithm 2

Input: $\{m_{l,e,k}(t), \forall l \in L, \forall k \in K\}$
Output: $\{x_{b,l}(t), \forall b \in B_e, \forall l \in L\}$

```

1 for  $k = 1$  to  $|K|$  do
2    $u_k(t) \leftarrow \sum_{l=1}^{|L|} m_{l,k}(t) - |\Psi_k^K|$ 
3 end
4 for  $f = 1$  to  $|F|$  do
5   for  $k$  in  $\Phi_f^F$  do
6      $i \leftarrow |R|$ 
7     while  $u_k(t) > 0$  and  $i \geq 0$  do
8       if  $m_{i,k}(t) \leq u_k(t)$  then
9          $u_k(t) \leftarrow u_k(t) - m_{i,k}(t)$ 
10         $m_{i,k}(t) \leftarrow 0$ 
11       else
12          $u_k(t) \leftarrow 0$ 
13          $m_{i,k}(t) \leftarrow m_{i,k}(t) - u_k(t)$ 
14       end
15       Try to first move  $\min(u_k(t), m_{i,k}(t))$  requests to racks in  $\Phi_f^F$ 
16       If it is not possible, move them to the racks in the other MSBs.
17        $i \leftarrow i - 1$ 
18     end
19   end
20 end
21 for  $k = 1$  to  $K$  do
22   for  $b$  in  $\Psi_k^K$  do
23     if  $\alpha_b(t-1) == 1$  and  $m_{\alpha_b(t-1),k} > 0$  then
24        $m_{\alpha_b(t-1),k} \leftarrow m_{\alpha_b(t-1),k} - 1$ 
25        $x_{b,\alpha_b(t-1)}(t) \leftarrow 1$ 
26     else
27     end
28   end
29 end

```

Algorithm 5: Training the PPO agent

```

1 Initialize the size of the memory, learning rate, etc.
2 Initialize one agent or  $|E|$  agents
3 for  $e = 1$  to  $|E|$  do
4   Start training the  $e$ -th agent if this is for the parallel agents case
5   for  $episode = 1$  to  $\Gamma$  do
6     Initialize the capacity requests, reservations, and servers
7     for  $t = 1$  to  $\mathcal{T}$  do
8       for  $l = 1$  to  $|L|$  do
9         Combine the information of the environment and actions of reservations  $1, \dots, l-1$ , into  $s_{l,e}(t)$ 
10        Send  $s_{l,e}(t)$  to the PPO agent and get  $\mathbf{a}_{l,e}(t)$ 
11        Convert  $\mathbf{a}_{l,e}(t)$  to numbers of servers to take by reservation  $l$ ,  $\{n_{l,e,f}(t), \forall f \in F\}$ , by (19)
12        Get numbers of servers to take from the racks,  $\{m_{l,e,k}(t), \forall l \in L, \forall k \in K\}$ , by Algorithm 3
13      end
14      Get server-to-reservation mapping,  $\{x_{b,l}(t)\}$  for all  $b$  and  $l$  by Algorithm 2
15      for  $l = 1$  to  $|L|$  do
16        Calculate the reward of reservation  $l$  by (3)
17        Store the state, action, and reward in the memory of the PPO agent
18      end
19      Update the environment with the server-to-reservation mapping,  $\{x_{b,l}(t), \forall b \in B, \forall l \in L\}$ 
20       $t \leftarrow t + 1$ 
21    end
22  end
23 end
24
25 end
26

```
